

# Novel application of satellite and in-situ measurements to map surface-level NO<sub>2</sub> in the Great Lakes region

C. J. Lee<sup>1</sup>, J. R. Brook<sup>2</sup>, G. J. Evans<sup>1</sup>, R. V. Martin<sup>3,4</sup>, and C. Mihele<sup>2</sup>

<sup>1</sup>Southern Ontario Centre for Atmospheric Aerosol Research, Department of Chemical Engineering and Applied Chemistry, University of Toronto, Toronto, Ontario, Canada

<sup>2</sup>Air Quality Research Division, Science and Technology Branch, Environment Canada, Downsview, ON, Canada

<sup>3</sup>Department of Physics and Atmospheric Science, Dalhousie University, Halifax, Nova Scotia, Canada

<sup>4</sup>Harvard-Smithsonian Center for Astrophysics, Cambridge, MA, USA

Received: 12 March 2011 – Published in Atmos. Chem. Phys. Discuss.: 21 June 2011

Revised: 28 October 2011 – Accepted: 10 November 2011 – Published: 24 November 2011

**Abstract.** Ozone Monitoring Instrument (OMI) tropospheric NO<sub>2</sub> vertical column density data were used in conjunction with in-situ NO<sub>2</sub> concentrations collected by permanently installed monitoring stations to infer 24 h surface-level NO<sub>2</sub> concentrations at 0.1° (~11 km) resolution. The region examined included rural and suburban areas, and the highly industrialised area of Windsor, Ontario, which is situated directly across the US-Canada border from Detroit, MI. Photolytic NO<sub>2</sub> monitors were collocated with standard NO<sub>2</sub> monitors to provide qualitative data regarding NO<sub>z</sub> interference during the campaign. The accuracy of the OMI-inferred concentrations was tested using two-week integrative NO<sub>2</sub> measurements collected with passive monitors at 18 locations, approximating a 15 km grid across the region, for 7 consecutive two-week periods. When compared with these passive results, satellite-inferred concentrations showed an 18% positive bias. The correlation of the passive monitor and OMI-inferred concentrations ( $R=0.69$ ,  $n=115$ ) was stronger than that for the passive monitor concentrations and OMI column densities ( $R=0.52$ ), indicating that using a sparse network of monitoring sites to estimate concentrations improves the direct utility of the OMI observations. OMI-inferred concentrations were then calculated for four years to show an overall declining trend in surface NO<sub>2</sub> concentrations in the region. Additionally, by separating OMI-inferred surface concentrations by wind direction, clear patterns in emissions and affected down-wind regions, in particular around the US-Canada border, were revealed.

## 1 Introduction

Nitrogen oxides (NO<sub>x</sub>), composed of nitric oxide (NO) and nitrogen dioxide (NO<sub>2</sub>) are an important family of atmospheric pollutants (NO<sub>x</sub> = NO + NO<sub>2</sub>). The main source of NO<sub>x</sub> in Ontario, Canada is transportation, with a smaller component originating from electricity generation and industrial processes (MoE, 2008). Other sources of NO<sub>x</sub> include soil and lightning. NO<sub>2</sub> has been used as a marker for vehicle emissions and has thereby been associated with adverse human health effects (Brook et al., 2007; Jerrett et al., 2009; Clark et al., 2010; Lenters et al., 2010). In the province of Ontario, Canada, the government guideline exposure limit for NO<sub>2</sub> is 100 ppb averaged over 24 h and 200 ppb averaged over 1 h. Despite the association of NO<sub>2</sub> with adverse health outcomes, and its utility as a marker for traffic and/or combustion pollution, NO<sub>2</sub> monitoring networks remain sparse.

NO<sub>2</sub> is commonly measured by chemiluminescence (CL) monitors which work by reducing NO<sub>2</sub> to NO and measuring the light produced by titrating the NO with O<sub>3</sub>. There are a number of methods for reducing the NO<sub>2</sub>, the most common being a heated molybdenum surface, which becomes oxidized to MoO<sub>2</sub> and MoO<sub>3</sub> and must be periodically recharged. We will refer to this type of monitor as MoO. These monitors are known to suffer from interference due to other oxidized nitrogen species NO<sub>z</sub> (NO<sub>z</sub> = HNO<sub>3</sub> + HONO + N<sub>2</sub>O<sub>5</sub> + RONO<sub>2</sub> + ...), since the heated molybdenum surface exhibits low selectivity (Winer et al., 1974; Steinbacher et al., 2007). This interference can especially be a problem in rural areas with low NO<sub>2</sub> concentrations and high NO<sub>z</sub> due to aged air masses or high organic concentrations. Photolytically converted CL monitors do not suffer from this interference (Ryerson et al., 2000). These



Correspondence to: C. J. Lee  
(colinj.lee@utoronto.ca)

photolytic monitors operate on essentially the same principle as the MoO-CL monitors, however, the NO<sub>2</sub> is reduced by applying intense light at ~420 nm which is specific to NO<sub>2</sub> and therefore is expected to produce almost no interference from other oxidized nitrogen species.

Due to the low relative per-monitor cost, NO<sub>2</sub> has also been measured using networks of passive monitors. For example, the networks have been used to assess human exposure to traffic related air pollution at high spatial resolution (Jerrett et al., 2009). These passive monitors consist of a chemically treated filter pad placed in a protective housing and exposed to ambient air for a period of time, usually two or more days. At the end of the sampling period, the filter is removed and the treatment is dissolved off the filter and analyzed using ion chromatography. Although the filters themselves are inexpensive, the method is labour intensive. As well, since there are no pumps, the exposure, and therefore the collection efficiency, is influenced by local meteorology.

Beginning with the Global Ozone Monitoring Experiment (GOME) in 1995, satellite-based spectroscopic measurements of atmospheric NO<sub>2</sub> have been taken by a series of instruments (Bovensmann et al., 1999; Burrows et al., 1999; Levelt et al., 2006). The Ozone Monitoring Instrument (OMI), launched in 2004 aboard the Aura satellite, has provided near daily-global NO<sub>2</sub> column measurements at unprecedented spatial resolution. Many recent works have compared OMI NO<sub>2</sub> columns with measurements provided by in situ surface monitors (Kramer et al., 2008; Boersma et al., 2009), long-path surface measurements (Kramer et al., 2008) and in situ aircraft measurements (Bucselá et al., 2008). Recent validation studies indicate that biases in the satellite retrievals remain and must be addressed when interpreting the data (Hains et al., 2010; Herron-Thorpe et al., 2010; O'Byrne et al., 2010; Lamsal et al., 2010). It is also important to note that a number of different data products with significant differences exist, adding to the complexity of comparisons between OMI and in-situ data.

Lamsal et al. (2008) used GEOS-Chem, a global chemical transport model (CTM), to infer ground level concentrations from OMI NO<sub>2</sub> data and showed good agreement between OMI overpass measurements and 2 h averages from a large network of ground monitors over the continental US and Canada with a mean difference of -18 % (urban) to 11 % (rural) between OMI inferred concentrations and corrected surface monitor data during the summer and fall seasons. Other studies such as Boersma et al. (2009) and Russell et al. (2010) have examined spatial and temporal characteristics of NO<sub>2</sub> over smaller regions such as Israel and California. Additionally, satellite NO<sub>2</sub> measurements were found to agree well with surface-level column measurements taken by MAX-DOAS as part the BAQS-met campaign (Halla et al., 2011). These analyses indicate that insight into the spatial distribution of ground-level NO<sub>2</sub> at a regional-to-local scale on the Earth's surface can be achieved with satellite remote sensing.

These high resolution OMI column density measurements also have been applied to constrain emissions. For example, Boersma et al. (2007) conducted an inversion using GEOS-Chem to infer emissions for the Eastern United States and Mexico and differences between these OMI-constrained top-down inventories and the US EPA National Emissions Inventory for 1999 (NEI99) were further used to infer changes over time to emissions from specific sectors. This was possible due to the geographic separation of the different sectors' emissions and the fine spatial resolution of the OMI-constrained top-down inventories. OMI column data has also been used to help verify and develop a regional chemistry model with 15 km resolution around the state of California (Kim et al., 2009). The weekend effect was also observed and contrasted between different cities in California using OMI vertical column densities from multiple years averaged on a 0.025° (~3 km) grid (Russell et al., 2010).

High-resolution estimates of surface concentrations can provide a number of contributions to air quality research:

- to closely examine urban impacts on surrounding rural regions,
- to improve estimates of chronic human and ecosystem exposure patterns,
- to look at transboundary flow of NO<sub>x</sub> which has been used as a combustion tracer when close to the source of combustion,
- to evaluate high-resolution air quality models (e.g., Makar et al., 2010).

The BAQS-met campaign was conducted in Southwestern Ontario, around the Windsor-Detroit area, from 1 June to 10 September 2007. The main goal of BAQS-met was to study the effects of transboundary air pollution and the Great Lakes meteorology on local air quality. The area was chosen due to its unique geography (i.e. frequent influence of lake breezes), proximity to the US-Canada border and local industry. A comprehensive suite of measurements, which have been described in other papers in this special issue (e.g., Levy et al., 2010) and included a diverse and relatively dense array of surface NO<sub>2</sub> measurements, provided a unique opportunity to develop and evaluate OMI-derived surface NO<sub>2</sub> concentration estimates.

In situ NO<sub>2</sub> routine monitoring data are publicly available. However, these monitors are sparsely-spaced, point measurements. It is therefore difficult to provide an accurate representation of NO<sub>2</sub> concentrations in between monitoring stations. The objectives of the work in this paper are thus to develop an approach to use OMI tropospheric column data to estimate spatially resolved surface NO<sub>2</sub> concentrations at a regional-to-local scale and then to provide examples of the insights that can be gained regarding spatial and temporal patterns of surface NO<sub>2</sub> in the study region.

As discussed above, a major contribution of previous work in this area was the use of a CTM to estimate a surface-concentration-to-column-density ratio which was applied to satellite NO<sub>2</sub> columns for this purpose (Lamsal et al., 2008). We hypothesized that this ratio could be calculated using publicly available data from a network of permanent surface monitoring stations in place of the CTM, in regions with sufficient ground-based monitors. This approach has the advantage of simplicity since it is not dependent upon CTM runs. Another potential advantage to this method is the empirical nature by which it is calculated, making it less sensitive to the OMI data product used. This claim is explained further in Sect. 2.3.

Because of the nature of the BAQS-met campaign setup, several important facets of our hypothesis could be examined and are reported in this paper. The estimated surface NO<sub>2</sub> results were compared with passive NO<sub>2</sub> measurements obtained at 18 locations for each of 7 sampling periods. Since the passive sites were spaced as closely as 15 km and were not used to calculate the ratio (i.e., were independent), they were well-suited for determining the accuracy of the estimated concentrations on a spatial scale not yet examined, across a variety of land-use types spanning from urban to rural locations. The collocated conventional and photolytic NO<sub>2</sub> monitors allowed for quantification of the NO<sub>2</sub> interference known to impact conventional measurements. Additionally, it was possible to examine the diurnal patterns in the interference and to assess the impact of these patterns on the comparison of the 14-day integrated passive NO<sub>2</sub> with the 14-day average OMI NO<sub>2</sub> based upon the midday overpasses. Finally, because of the additional rural chemiluminescence monitoring provided during the campaign, the value of these more spatially representative rural monitoring sites for improving the exploitation of the freely available OMI satellite observations could be highlighted.

To the best of our knowledge, the simple approach we develop and evaluate here for combining in-situ data from permanent monitoring stations with high-resolution satellite data to obtain high-resolution (~ 11 km) estimates of long-term average surface NO<sub>2</sub> concentration maps has not been considered before. In addition, the region covered and the 15 km spacing of the passive monitors allowed for an unprecedented surface NO<sub>2</sub> dataset against which to compare the maps generated using this novel method. Furthermore, the use of two-week passive samplers for evaluation provides a baseline which is expected to be more representative of chronic human-exposure conditions, therefore increasing the relevance of this study to the health research community.

## 2 Measurements of Windsor and Southwest Ontario area NO<sub>2</sub>

Windsor, Ontario, is located at the southwestern tip of the province of Ontario. It is bordered by the Detroit River on the

west side and Lake St. Clair to the north, as well as Lake Erie several km to the south. This type of waterfront geography can have effects on NO<sub>2</sub> concentrations due to lake breezes (Arain et al., 2009). Across the Detroit river lies Detroit, MI. Both cities are known for their auto industry. The Windsor metropolitan area has a population of 323 000 and an area of 1023 km<sup>2</sup>, while the City of Windsor has a population of 216 500 and occupies an area of 147 km<sup>2</sup> (Statistics Canada, 2006). Southeast Michigan, including Detroit-Warren-Flint, is the eleventh most populous combined statistical area in the US with a population of 5 300 000 and an area of 15 000 km<sup>2</sup> (US Census Bureau).

### 2.1 High-time resolution measurement by chemiluminescence

The Ontario Ministry of the Environment (MoE) operates a permanent monitoring network which includes 2 stations within Windsor and one in Chatham (Fig. 1). Due to their proximity to the campaign area, MoE permanent monitoring sites in Sarnia, at the Southern end of Lake Huron, and London, approximately 150 km Northeast of Windsor, were also included (Fig. 2). As well, during the intensive campaign period (20 June–10 July 2007) 3 additional chemiluminescence (CL) monitors were set up at Harrow and Ridgetown, on the North shore of Lake Erie approximately 40 km and 100 km from Windsor, respectively, and on Pelee Island, a 42 km<sup>2</sup> island approximately 50 km Southeast of Harrow in Lake Erie (Fig. 1). The monitors operated by MoE were Thermo TE42C instruments which provide NO, NO<sub>2</sub> and NO<sub>x</sub>. Measurements were averaged to 1 h to match the data available from the permanent MoE network.

To evaluate the potential interference from non-NO<sub>2</sub> oxidized nitrogen species (Steinbacher et al., 2007; Ordóñez et al., 2006; Lamsal et al., 2008), 3 CL monitors (TE42C and TE42CTL) were deployed by Environment Canada for the duration of the campaign (1 June 2007 to 11 September 2007). One of these monitors was located at Bear Creek, collocated with a MoO-CL monitor; one was located at Harrow; and one (which was not used in this analysis) was onboard the Environment Canada mobile platform, CRUISER. These CL monitors were each equipped with a photolytic converter (Droplet Measurement Technologies, blue light converter) and an external molybdenum converter. By selecting ambient air, photolytically converted air, or molybdenum converted air, true NO<sub>2</sub> could be reported by subtracting NO from the measured post-conversion NO and applying the conversion efficiency of NO<sub>2</sub> to NO. One minute concentrations for NO, NO<sub>2</sub> and NO<sub>y</sub> (NO<sub>y</sub> = NO<sub>x</sub> + NO<sub>2</sub>) were provided by running a 1 min cycle with the three above channels and 2 internal zeros.

It is important to highlight that the method for measuring NO<sub>y</sub> is exactly the same as the method commonly used for measuring NO<sub>2</sub> with the exception that in traditional atmospheric NO<sub>2</sub> monitoring, the converter is internal to the

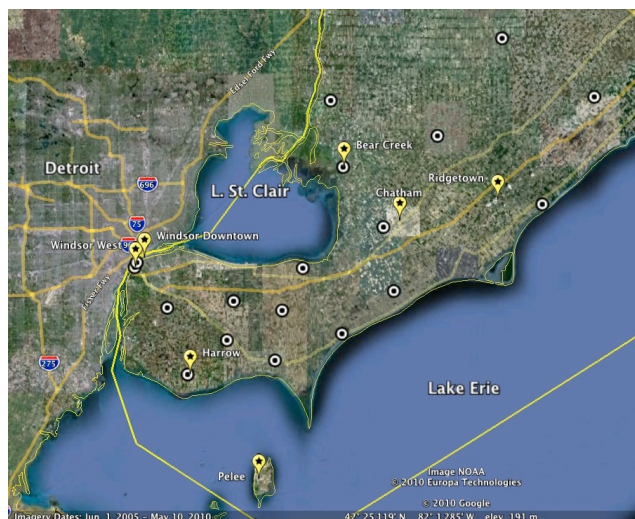


**Fig. 1.** NO<sub>2</sub> monitoring sites for the 2007 BAQS-Met campaign. Passive monitoring locations are denoted by black-and-white circles. High-time resolution chemiluminescence monitor locations are marked by yellow bubbles with text labels. Chatham, Windsor West and Windsor Downtown were Ontario Ministry of the Environment (MoE) permanent monitoring stations. Harrow, Pelee and Ridgeway also had monitors operated by MoE from 20 June to 10 July. Harrow had a photolytically converted chemiluminescence monitor operated by Environment Canada from 1 June to 10 September and Bear Creek had both molybdenum and photolytically converted monitors operated by Environment Canada for the same period. Two additional MoE permanent monitoring station not shown by this map were also used (Sarnia and London).

monitor. The NO<sub>2</sub> interference in MoO NO<sub>2</sub> measurements is therefore a product of the conversion efficiency of the constituent species of NO<sub>2</sub> as well as their respective line loss parameters (HNO<sub>3</sub> is particularly noted for line losses, Steinbacher et al., 2007). In the NO-NO<sub>2</sub>-NO<sub>y</sub> setup used for measuring the interference, the MoO converter was applied before the sampling line and NO<sub>y</sub> measurement was dependent only on the conversion efficiencies of the species.

## 2.2 Measurement by passive monitor

A network of passive NO<sub>2</sub> monitors was deployed at 18 locations (Fig. 2). These sites were part of the Mesonet study (Levy et al., 2010) and were chosen to closely match the Environment Canada Global Environmental Multiscale model (Makar et al., 2010) meteorological forecast 15 km model grid in the region (every grid point where possible, alternate grid points in other locations). In some cases the need to access the monitors on a regular basis caused small deviations from the model grid. Weatherproof housings were anchored to the Mesonet towers at the sampling sites. These housings were designed to allow ambient air contact with the monitors while keeping out rain.

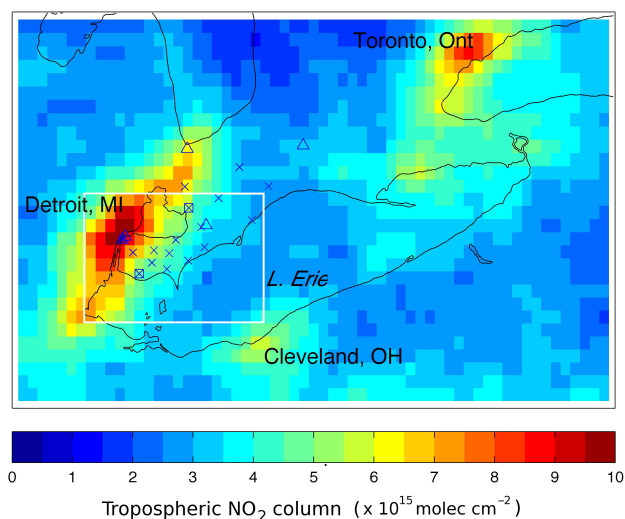


**Fig. 2.** Campaign average NO<sub>2</sub> column in Southwestern Ontario. BAQS-met passive monitoring sites are marked by Xs, triangles represent permanent MoE molybdenum converted NO<sub>x</sub> monitoring locations and squares denote locations of EC photolytically converted NO<sub>x</sub> monitors during the campaign. White rectangle outlines area encompassed by Fig. 1.

Further, since the filters needed to be collected for analysis and replaced with fresh samplers manually, site locations were selected with the criterion that all sites could be reached in a single day. The intention was to provide consistent sampling period start and end dates across all sampling periods. However, this was not always possible and some sites saw collection and replacement up to two days before others, although most sites were collected and replaced on the same day in most cases. In total, there were 115 passive samples collected: the first 6 periods (31 May to 22 August) had 17 simultaneous sampling sites and the final period (23 August to 6 September) had 13 sampling sites. On average, 70% of the filters were collected on a single day, thus maximizing temporal overlap for the two-week period. For sampling periods 1 and 3 through 7, all filters were collected within a 2 day period; for sampling period 2, all filters were collected within a 2 day period, except one filter which was collected 2 days later than the first.

Paired filters were deployed at each sampling location to ensure data quality and consistency of results. Collocated filters were checked for consistency and if values differed by more than 10% the two measured concentrations were subjected to additional quality assurance checks including examination of the chromatograms and possible reanalysis to improve the IC results and, if acceptable after these changes (within 20%), the two values were averaged. However, if one of the two was still found to be an outlier or contaminated then it was excluded from the averaging. In the case of a known source of error, one filter was rejected and the site value was reported from only the good filter. Multiple

unexposed filters, carried to and from the sampling locations during the campaign, were used for background/blank correction.

### 2.3 Satellite remote sensing

The OMI instrument is onboard the Earth Observing System (EOS) Aura satellite which is in a sun-synchronous orbit with south-north Equator crossing of 13:45 LT (Levelt et al., 2006). OMI is carried aboard the Earth Observing System. With a wide field-of-view and sun-synchronous orbit, the instrument was designed to provide daily coverage across most of the globe. The sensor observes 60 pixels which together cover a swath 2600 km wide, perpendicular to the direction of travel. The satellite travels at approximately 7 km s<sup>-1</sup> ground speed and each exposure is roughly 2 s long, resulting in each row covering 13 km on the ground in the along-track direction. Across track, pixels are 24 km wide at nadir, but due to geometry, nearer the edge of the swath, pixels can be as wide as 150 km. Recently, obstruction of parts of the sensor has limited measurements slightly, removing as many as 18 pixels out of the 60.

Two commonly used, publicly available data products generated from the raw data collected by OMI are: the Standard Product (SP) provided by NASA (Bucsela et al., 2006, [http://disc.sci.gsfc.nasa.gov/Aura/data-holdings/OMI/omno2\\_v003.shtml](http://disc.sci.gsfc.nasa.gov/Aura/data-holdings/OMI/omno2_v003.shtml)), and the DOMINO Product provided by the Tropospheric Emissions Monitoring Internet Service (TEMIS) (Boersma et al., 2007, <http://temis.nl/airpollution/no2.html>). Both data products begin by using the DOAS algorithm to fit the absorption spectrum of NO<sub>2</sub> to the measured spectrum of backscattered 405 to 465 nm solar radiation (Boersma et al., 2007). The contribution of stratospheric NO<sub>2</sub> is then removed (Bucsela et al., 2006; Boersma et al., 2007). The air mass factor (AMF) accounts for viewing geometry and light-scattering interferences such as clouds; this AMF is applied to convert the measured slant columns into tropospheric vertical column densities. It is these conversions that introduce the most uncertainty in the reported vertical columns over polluted areas (Boersma et al., 2007, 2004; Martin et al., 2002).

The use of in situ data to determine the surface-to-column NO<sub>2</sub> relationship makes this analysis insensitive to potential bias in the OMI NO<sub>2</sub> data. Starting with the DOMINO product, a tropospheric slant column destripping process was used to remove scan-angle dependent bias (Celarier et al., 2008; Lamsal et al., 2010), using a 24 h history to compute single-scan position biases. Pixels with cloud radiance fractions greater than 0.3 were rejected, as were pixels near the edge of the swath (width > 50 km). The resulting vertical column densities easily identified the urban areas as major NO<sub>x</sub> sources (Fig. 2).

Whereas in situ measurements are true surface measurements, OMI tropospheric NO<sub>2</sub> vertical column density measurements include both the surface-level NO<sub>2</sub> and its vertical

distribution through the tropospheric column. This distribution depends on the chemical lifetime of NO<sub>x</sub>, the partitioning of NO<sub>x</sub> into NO and NO<sub>2</sub>, layering of the atmosphere and the dispersion of NO<sub>x</sub> during vertical mixing. Lamsal et al. (2008) inferred surface-level NO<sub>2</sub> concentrations ( $S$ ) from OMI tropospheric vertical column densities ( $\Omega$ ) by applying the ratio of surface-level NO<sub>2</sub> concentrations ( $S_G$ ) to vertical column densities ( $\Omega_G$ ) calculated using the GEOS-Chem global CTM:

$$S = \frac{S_G}{\Omega_G} \times \Omega \quad (1)$$

In order to obtain surface concentrations without the use of a CTM, we determined the spatial average ratio of in situ surface concentration ( $\bar{S}$ ) to OMI columns ( $\bar{\Omega}$ ), coincident with surface monitoring stations, over the region (Eq. 2),

$$S = \frac{\bar{S}}{(\bar{\Omega} - \Omega_{BG})} \times (\Omega - \Omega_{BG}) \quad (2)$$

where  $\Omega_{BG}$  is the background OMI NO<sub>2</sub> column as described in the subsequent paragraph.

To account for the larger fractional contribution of the free troposphere in areas with low surface concentrations, all pixels (after filtering) in the region contained by the boundary of Fig. 2 were sorted by column density for each overpass. The lowest decile value (i.e., the value separating the bottom 10 % of the data from the remaining 90 % of pixels) was subtracted from every pixel in the overpass. This allowed for the free-tropospheric component to be accounted for ( $\Omega_{BG}$  in Eq. 2), while limiting sensitivity to the uncertainty of any single pixel. The mean value of the free-tropospheric column during the campaign period was  $0.8 \times 10^{15}$  molec cm<sup>-2</sup>. This process did result in negative (i.e., below detection) values, but they were typically small and constrained to the northernmost areas of the region.

Each single-pixel measurement carries with it an uncertainty due to the spectral fitting, surface albedo, cloud cover and air mass factor. This uncertainty can reach up to 40 % in heavily polluted areas (Boersma et al., 2007), including the locations of some of the high-time resolution in situ monitors used to calculate the surface-to-column ratio. In addition to this, an OMI pixel is an average over a large area on the surface of the Earth while the in situ monitors measure at a specific location which is not necessarily representative of the entire pixel area against which is being compared. We therefore generated an average surface-to-column ratio for the entire region by averaging the ratios observed at several surface monitoring stations. Implicit to this approach was the assumption that this ratio varies temporally (i.e., day-to-day) but not spatially across the region on any given day. The error in this assumption is discussed in Sect. 3.3.1.

To generate the inferred surface concentration map for a given overpass, every pixel from the overpass ( $\Omega$  in Eq. 2), minus the free-tropospheric contribution, was multiplied by

this average ratio ( $\frac{\bar{S}}{\bar{\Omega} - \bar{\Omega}_{BG}}$  in Eq. 2) to provide a region-wide snapshot of surface NO<sub>2</sub> concentrations at overpass time. This procedure was analogous to Eq. (4) from Lamsal et al. (2008), which also accounts for the contribution of the free troposphere. Equation (4) from Lamsal et al. (2008) also provides higher resolution than the available GEOS-Chem 2° × 2.5° resolution using a ratio of local OMI columns to the average OMI column for the entire grid cell. This suggests that by using a single ratio for the entire region for each overpass, an error of up to ±35 % is introduced in rural areas.

From Eq. (2), it can be seen that the use of in situ data to determine the surface-to-column NO<sub>2</sub> relationship makes this analysis insensitive to potential bias in the OMI NO<sub>2</sub> data. Because OMI column densities appear in both the numerator and the denominator, any bias present in the particular retrieval used would be expected to cancel out. As an example, it has been suggested that the SP is biased low in the winter (Lamsal et al., 2008). If the surface-to-column ratio is calculated using the (assumed, in this case, unbiased) modeled surface concentration and modeled column density, the inferred surface values from these low OMI columns will also be biased low. However, by calculating the ratio using the observed OMI columns, assuming the in-situ measured surface concentration is the same as the modeled surface concentration, the surface-to-column ratio will be greater than the modeled surface-to-column ratio which will increase the final inferred surface concentrations.

For comparison of OMI column densities and surface concentrations with long-term time-averaged passive monitor results, OMI measurements were resampled on a 0.1° × 0.1° grid. Each grid cell was then given a weight proportional to the inverse of the area of the pixel which contained that grid cell. This had the effect of giving near-nadir pixels higher weight than pixels closer to the swath edge. These regridded measurements were then averaged over two weeks using these weights, providing a long-term average to compare with in situ passive monitor measurements. Although this weighting scheme has also been used with a squared-uncertainty term (Wenig et al., 2008), it was found that inverse-area-alone weighted values used here differed from inverse-area, inverse-squared-uncertainty weighted values by less than 3 % for the 2-week averages over the campaign period.

## 3 Results and discussion

### 3.1 Characterising surface NO<sub>2</sub>

#### 3.1.1 Spatial and temporal patterns inferred from chemiluminescence monitor data

NO<sub>2</sub> concentrations were found to vary both spatially and temporally. The hourly and daily concentrations of NO<sub>2</sub> showed moderate to weak correlations between the sites

over the duration of the campaign (Table 1). This comparison is important to help identify potential sources of pollution affecting different areas of the campaign region, which spans urban, rural and industrial areas. Ridgetown showed a relatively high correlation with the urban sites (~0.7), which was surprising because Ridgetown is over 100 km from the urban and industrial centre of Windsor. However, the Ridgetown measurement site was 5 km from highway 401, a major provincial highway in the region leading directly to the Ambassador Bridge border crossing in Windsor. This relatively strong correlation despite the spatial separation implied that 401 traffic was an important source in both of these areas.

NO<sub>2</sub> concentrations varied diurnally and day-to-day at both the urban (Windsor) and rural (Harrow, Bear Creek) sites (Fig. 3). Peak concentrations for Windsor occurred between 06:00 and 10:00 a.m. (local standard time) on most days, while these morning rush-hour peaks were sometimes delayed at the rural sites downwind. Variation between sites was greater than week-to-week variations in same-site NO<sub>2</sub> concentrations (Table 2). The largest between-site ratio in the median weekly concentration was over 4 (Windsor Downtown had a weekly median concentration of 13.6 ppb while Peelee had a weekly mean of only 2.9 ppb) whereas the largest ratio between maximum and minimum weekly concentrations at a single site was less than 2 (Peelee had the highest ratio with a maximum weekly concentration of 3.1 ppb and a minimum of 1.7 ppb). In contrast, daily averages varied about as much at a given site as they did between sites. This indicated that spatial distributions remain fairly stable over the region, even though local events may briefly increase the spatial heterogeneity. This result is important for high spatial resolution interpretation of satellite remote sensing data because these methods take advantage of differences in the daily footprint of the instrument overpass to extract long-term patterns in spatial air pollution distributions.

#### 3.1.2 Passive monitor results

Campaign average NO<sub>2</sub> measurements recorded at the passive monitoring sites ranged from a minimum site average of 3.3 ppb (rural) to a maximum of 18.8 ppb (urban). The passive monitors also revealed that over the long-term the magnitude of the spatial variability was greater than the magnitude of the differences between time periods at a given location. This is exemplified in Fig. 4, comparing the concentrations measured at each location for sampling period 6 (7 August to 21 August) to the campaign average concentration at each sampling site. In fact, the minimum correlation coefficient between a single sampling period and the campaign average was observed during period 6 ( $R = 0.97$ ); all other sampling periods correlated with campaign averages with  $R > 0.98$ , with a slope near 1. The maximum ratio between minimum and maximum two-week average NO<sub>2</sub> concentrations at any given site was 1.8, while the ratio between the

**Table 1.** Correlation (Pearson *R*) between NO<sub>2</sub> measurement sites during the BAQS-met campaign (1 June to 10 September, 2007). The first row for each location represents the correlation between hourly measurements while the second represents correlation between daily measurements. All monitors not marked with a \* were heated molybdenum converted chemiluminescence monitors while those marked with a \* were photolytically converted chemiluminescence monitors.

Site	Harrow (MoE)	Ridge-town	Windsor West	Windsor Downtown	Chatham	Harrow (EC)*	Bear Creek*
Pelee	0.49	0.43	0.51	0.51	0.46	0.41	0.36
	0.54	0.35	0.63	0.60	0.54	0.35	0.43
Harrow (MoE)		0.48	0.50	0.49	0.47	0.95	0.46
		0.51	0.58	0.57	0.41	0.87	0.68
Ridgetown			0.71	0.68	0.59	0.42	0.55
			0.65	0.68	0.63	0.36	0.76
Windsor West				0.85	0.56	0.47	0.49
				0.83	0.39	0.41	0.50
Windsor Downtown					0.63	0.42	0.46
					0.50	0.32	0.44
Chatham						0.30	0.44
						0.17	0.47
Harrow (EC)*							0.37
							0.34

**Table 2.** Minimum, median and maximum observed 1-day and 1-week average NO<sub>2</sub> concentrations measured by chemiluminescence monitors during the BAQS-met campaign. All monitors not marked with a \* were heated molybdenum converted chemiluminescence monitors while those marked with a \* were photolytically converted chemiluminescence monitors.

Site	Daily			Weekly		
	Min (ppb)	Median (ppb)	Max (ppb)	Min (ppb)	Median (ppb)	Max (ppb)
Pelee	0.1	2.8	4.0	1.7	2.9	3.1
Harrow (MoE)	3.1	5.3	8.0	5.3	5.4	5.5
Ridgetown	2.5	5.8	7.1	4.8	5.0	6.0
Windsor West	5.5	13.2	22.9	10.8	12.9	15.2
Windsor Downtown	4.4	13.1	30.6	11.3	13.6	18.6
Chatham	2.2	7.0	13.7	5.6	7.2	7.6
Harrow (EC)*	2.6	4.5	7.9	3.7	4.8	5.4
Bear Creek*	1.1	2.9	6.1	2.4	3.1	4.1

highest site median value and the lowest site median value was 6.4. This result is consistent with the findings presented in Sect. 3.1.1, that long term spatial patterns remain relatively stable compared with the differences in concentration across the region. This also highlights the potential that midday satellite observations averaged over multiple days can have in capturing the spatial pattern.

A passive monitor was located at Harrow for the first 3 two-week sampling periods (1 June 2007 to 10 July 2007) as well as a photolytically converted CL monitor for the entire campaign and a MoO-CL monitor for the intensive cam-

paign (20 June to 10 July). Bear Creek had a passive monitor for the remaining 4 periods (11 July 2007 to 4 September 2007) along with both photolytically and MoO converted CL monitors. As well, the permanent MoE site (molybdenum converted NO<sub>2</sub>), Windsor West, had a passive monitor. The passive monitors were in reasonably good agreement with the collocated CL monitors (Fig. 5a). The average absolute difference between the passive and the MoO CL and the photolytic CL were 11 % and 15 %, respectively. The overall slope of the relationship was 1.04.

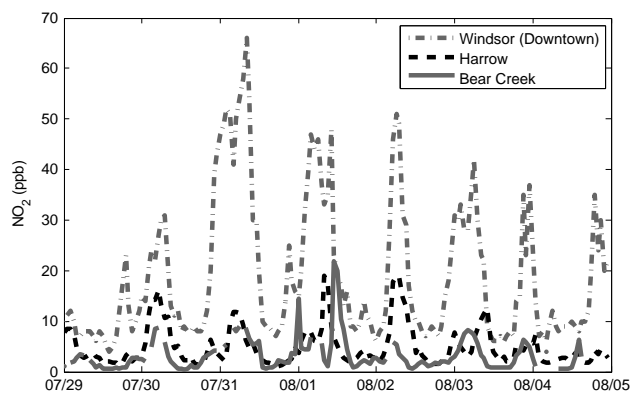


**Fig. 3.** NO<sub>2</sub> measured at 1 urban (Windsor) and 2 rural (Harrow, Bear Creek) locations during 1 week of the BAQS-met 2007 campaign. This week was selected as generally representative of patterns observed over the whole campaign. NO<sub>2</sub> concentrations can be seen to exhibit significant diurnal and day-to-day variation.

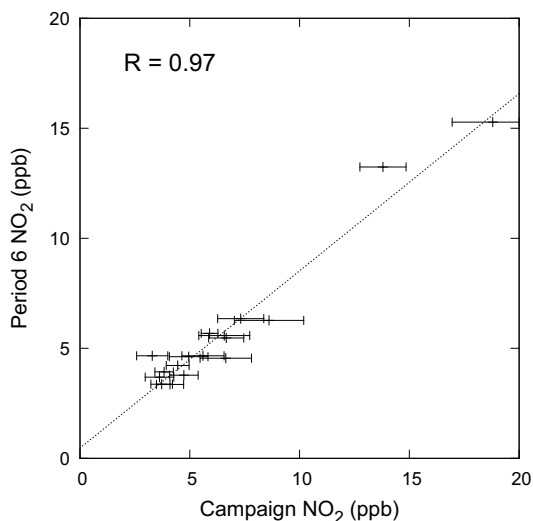


**Fig. 4.** Single sampling period average NO<sub>2</sub> concentration vs. same-site campaign average concentrations for sampling period 6 (7–21 August). Error bars show  $\pm 1$  standard deviation from same-site averages. This sampling period represented the lowest linear correlation against the average concentration.

Passive monitors provide time integrated averages while OMI only measures once daily, between 12:00 and 14:00 LT at this latitude. It was therefore important to understand how the average NO<sub>2</sub> values just around OMI overpass times (12:00 to 14:00 LT each day) relate to concentrations averaged over the two-week timescale of the passive monitor measurements. Although the slope was, as expected, substantially higher since the midday NO<sub>2</sub> values were lower than daily averages, the correlation remained strong (Fig. 5b). Similar results were obtained when daily average CL data were compared to midday averages from the same

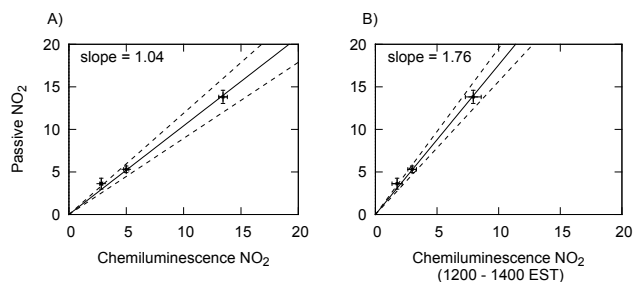


**Fig. 5.** Comparison of collocated passive and chemiluminescence monitors. X-error bars represent 95 % confidence intervals on averages from hourly data. Y-error bars represent 95 % confidence intervals on averages from approximately 2-week sampling period data.

monitors. This indicated that, with a suitable correction factor, OMI overpass averages could be adjusted so as to be representative of long-term integrated averages.

### 3.2 NO<sub>z</sub> interference

Much of the NO<sub>2</sub> monitoring data available are taken by MoO converted CL monitors. As indicated above, these converters are not specific to NO<sub>2</sub>, suffering from interference from other oxidized nitrogen species (NO<sub>z</sub>). Previous studies have reported MoO-converted CL NO<sub>2</sub> measurements to be as much as 2.3 times higher than simultaneous photolytically-converted CL measurements during summer months in a rural setting (Steinbacher et al., 2007). Quantifying this interference is important for the interpretation of satellite remote sensing data, which are specific to NO<sub>2</sub> and provide averages over large areas on the Earth's surface. Often satellite measurements are compared to rural monitors to ensure that the in situ data are representative of a wide local area and not affected by local sources (Lamsal et al., 2010). It is these rural monitors where the interference is expected to be the largest (Boersma et al., 2009).

In this study photocatalytic and heated molybdenum converted chemiluminescence monitors were collocated to evaluate the effects of NO<sub>z</sub> interference on the molybdenum converted measurements. All data was averaged to 1 h resolution, which corresponds with the resolution of the publicly available data for the permanent CL monitoring sites. At the Bear Creek (BC) site, the molybdenum-converted CL monitor hourly concentration was found to be 45 % ( $\pm 3$  %) higher, on average, than the photolytically-converted CL. The MoO measurements correlated strongly with the photolytic ( $R = 0.96$ ,  $n = 1472$ ), with a slope of 1.05 and an offset 0.65 ppb. This offset was responsible for the apparently large relative difference as the average NO<sub>2</sub> concentration for the site was only 2.9 ppb. When the difference between the two monitors was compared with NO<sub>z</sub> measurements taken by the photolytic monitor (Fig. 6), there was only a weak correlation ( $R = 0.26$ ,  $n = 1464$ ) with a slope of 0.11 and an

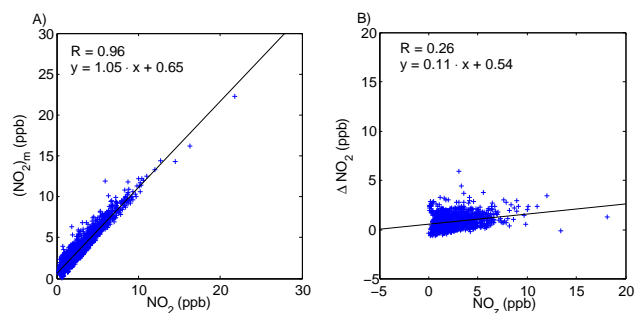


**Fig. 6.** (A) Comparison of collocated high-time resolution NO<sub>2</sub> measurements made by heated molybdenum converted (vertical axis) and photocatalytically converted (horizontal axis) chemiluminescence monitors. The solid line is the best-fit linear regression. (B) Comparison of difference between molybdenum converted and photocatalytic NO<sub>2</sub> measurements with NO<sub>z</sub> measurements (taken by BC2 monitor).

offset similar to that found when comparing the two sets of NO<sub>2</sub> measurements. Since the only difference between NO<sub>y</sub> as measured by the photolytic monitor and NO<sub>2</sub> measured by the molybdenum converted monitor was the point of conversion, the most likely explanation for the low slope and high offset is inlet deposition of NO<sub>z</sub> species. That is, about 90 % of the NO<sub>z</sub> is deposited on the way to the MoO CL monitor, but some of this is later released, resulting in NO<sub>z</sub> interference even in the absence of detectable ambient NO<sub>z</sub>. In the 3 locations where NO<sub>z</sub> measurements were available, mean NO<sub>z</sub> between noon and 14:00 EDT were found to be low (2.62 ppb and 3.22 ppb for rural locations and 2.62 ppb for urban), indicating that NO<sub>z</sub> concentrations (and therefore NO<sub>z</sub> interference) remain low across the entire campaign region.

The interference by NO<sub>z</sub> did show a diurnal trend (Fig. 7). The median ratio of the MoO-CL to photolytic-CL monitor data was around to 1.15 for hours between midnight and 08:00 a.m., with a rise towards the afternoon and a maximum of 1.97 for 01:00 p.m. LST, then back down to 1.0 from 06:00 p.m. to midnight. Because of the rural location chosen for this comparison, the high midday ratio was partly due to the low NO<sub>2</sub> concentrations observed around midday – while the ratio of the MoO-CL to the photolytic-CL measurements was almost 2, the median difference between the monitors was only 0.9 ppb for the same time (01:00 p.m. local). This is largely due to the relatively low NO<sub>2</sub> concentrations at the monitoring location. When only hours for which the average photolytic NO<sub>2</sub> concentration was greater than or equal to 1 ppb were considered, this 01:00 p.m. median ratio is reduced to 1.53. Thus, the interference by NO<sub>z</sub> could cause significant uncertainties (up to 97 %) if the OMI data were compared only to midday MoO CL in situ concentration data for rural areas. However, the goal of this study was to compare long-term average NO<sub>2</sub> concentrations with OMI mea-

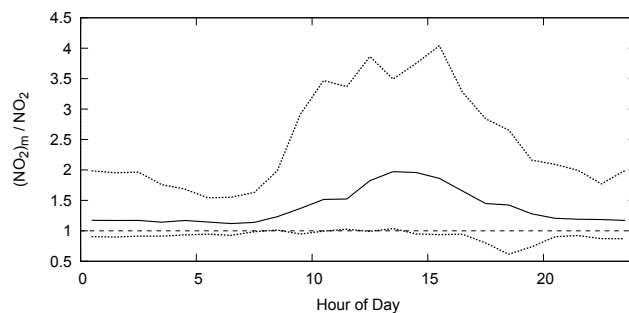


**Fig. 7.** Diurnal trend in ratio of (NO<sub>2</sub>)<sub>m</sub> to NO<sub>2</sub> measured from 1 June to 10 September, 2007 at Bear Creek, Ontario, a rural site located approximately 60 km northeast of downtown Detroit, MI. (NO<sub>2</sub>)<sub>m</sub> denotes NO<sub>2</sub> measured by heated molybdenum catalyst chemiluminescence monitor, which can suffer from interference due to reducing non-NO<sub>2</sub> oxidized nitrogen species. True NO<sub>2</sub> was measured by a collocated photolytic converted chemiluminescence monitor, which reduces NO<sub>2</sub> selectively. Solid line represents median ratio for that hour. Dotted lines represent 5th and 95th percentiles. Hours are Eastern Standard Time. OMI overpasses occur between 12:00 and 14:00 EST, which display some of the highest average ratios.

surements over a range of environments including rural areas with low concentrations and urban and industrial areas with higher NO<sub>2</sub> concentrations. Since all of the permanent monitoring locations (with MoO converted CL monitors) were in urban settings with higher average NO<sub>2</sub> levels, this 0.9 ppb median difference was deemed to be acceptable. Thus it was concluded that NO<sub>2</sub> data from the MoO-CL and photolytic-CL monitors could be combined and used for comparison with the OMI or passive monitor data.

### 3.3 Satellite observations

#### 3.3.1 Comparison with in situ passive measurements

Twenty-four hour surface NO<sub>2</sub> concentrations were estimated from OMI column data using the CL monitor data in conjunction with Eq. (2). The accuracy of the resulting ground-level spatial maps derived from this approach was evaluated by comparison with the passive monitoring data from the 17 sites. Without using Eq. (2), inverse-area-weighted averages of OMI tropospheric NO<sub>2</sub> vertical column measurements showed moderate correlation ( $R = 0.52$ ,  $n = 115$ ) with passive monitor concentrations. This was considered the baseline correlation, against which the inference method could be evaluated.

Qualitatively, OMI-inferred concentrations showed a similar geographical pattern to the passive monitoring network (Fig. 8). The highest concentrations were observed in the Detroit and Windsor urban areas with moderate values observed along the US-Canada border between Lake St. Clair and Lake Huron. The geographical pattern observed in the

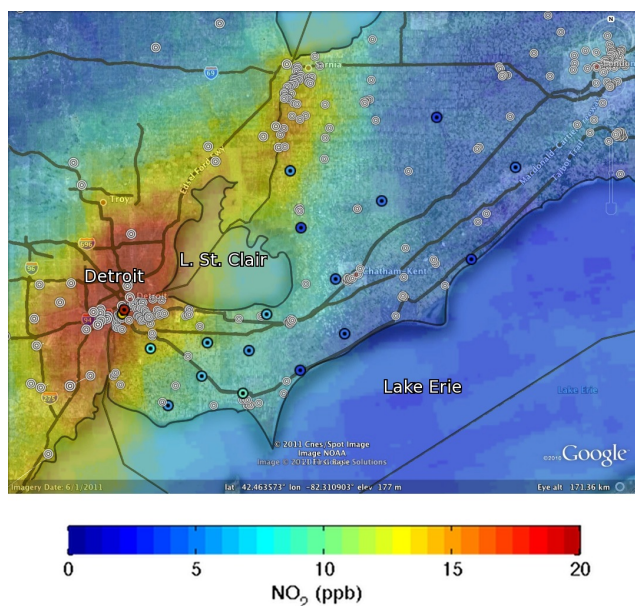


**Fig. 8.** Map of the campaign area with passive monitoring site campaign averages and emissions sources. Colour indicates OMI-inferred NO<sub>2</sub>. The passive sites are marked by coloured circles with the colour of the circle representing the campaign average NO<sub>2</sub> concentration (same colour scale as map). US EPA emissions sources with 2005 emissions greater than 100 t NO<sub>x</sub>/yr are marked on the US side, while Environment Canada NPRI emissions greater than 100 t NO<sub>2</sub>/yr are marked.

OMI-inferred NO<sub>2</sub> concentrations also follows the distribution of emissions sources with many of the NO<sub>2</sub> point sources, as reported by the Environment Canada National Pollutant Release Inventory and the United States Environmental Protection Agency. Figure 8 shows that many sources are clustered around the Detroit-Windsor urban area and along the border between Lake St. Clair and Lake Huron.

The procedure for calculating surface NO<sub>2</sub> from OMI columns was performed in two ways: once using the campaign-only NO<sub>2</sub> data in addition to the permanent MoE monitoring sites (7 sites total), and once using only the permanent MoE monitoring sites (5 sites). Correlation between OMI measurements and passive measurements improved from 0.52 using raw OMI NO<sub>2</sub> columns to 0.69, with a slope of 1.18, using the OMI inferred surface concentrations (Fig. 9). Interestingly, when only the MoE permanent monitoring stations were used, a correlation of 0.66 was obtained, but the slope increased from 1.18 to 1.32. The higher slope obtained when using only the five permanent MoE sites is attributed to their locations near NO<sub>x</sub> sources in urban sites. These in-situ NO<sub>2</sub> measurements are expected to be less representative of the overall pixel area whose average column is measured by OMI.

The surface-to-column ratios used to calculate OMI-inferred surface-level NO<sub>2</sub> concentrations varied somewhat

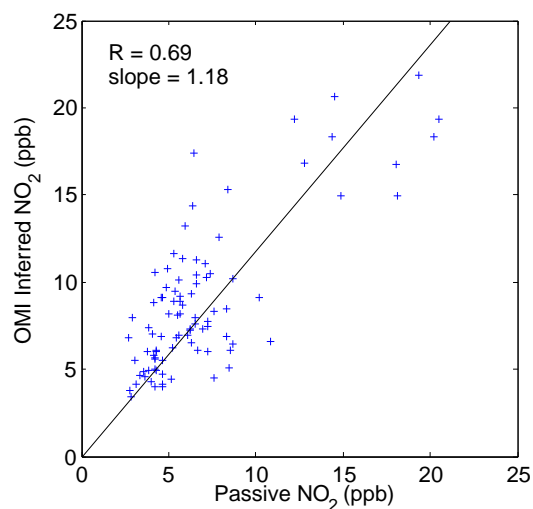


**Fig. 9.** Passive measurements taken during the BAQS-met campaign over 7 sampling periods at 17 simultaneous locations versus OMI inferred NO<sub>2</sub> concentrations at those same locations for the same periods.

across the 7 CL monitor sites with the lowest average ratio being 0.36 ppb/ $1 \times 10^{15}$  molec cm<sup>-2</sup> (i.e.,  $8.6 \times 10^{-6}$  cm<sup>-1</sup>) at the Environment Canada Bear Creek site and the maximum average ratio being 1.66 ppb/ $1 \times 10^{15}$  molec cm<sup>-2</sup> ( $4.0 \times 10^{-5}$  cm<sup>-1</sup>) at the MoE Chatham site. It is worth noting that the inverse of these surface-to-column ratios represents a characteristic height ( $H$ ) that varied from 250 to 1160 m. This metric provides a measure of the vertical extent of the NO<sub>2</sub>, assuming that the ground based measurement was representative of the OMI pixel.

In the case of the MoE Chatham site, the most likely local emission source is on-road vehicles. The urban area of Chatham itself is small ( $\sim 5$  km in diameter or 20 km<sup>2</sup>) and surrounded by rural areas. Thus, the surface NO<sub>2</sub> concentration within Chatham tends to be higher than that in the surrounding rural region. As a result, measurement at this MoE site is less representative of the area over which the OMI measurements are averaged, which is a minimum of 300 km<sup>2</sup>. Since most of the area included in the OMI pixel footprint is the surrounding rural area, as opposed to the urban area of Chatham, the high in situ concentration in Chatham and the low overall column density would result in a high surface-to-column ratio, as observed.

In the region upwind of the Bear Creek site there are a number of stack emissions sources (Fig. 8). Thus, NO<sub>2</sub> in this rural region has a higher potential to be above ground, compared to the vehicle emissions in Chatham. The low surface-to-column ratio determined for this site reflects this situation. The hypothesis of lofted NO<sub>2</sub> in this rural area is also borne out by the inferred NO<sub>2</sub> at the location of the passive monitor 18 km to the north of the Bear Creek monitoring site. At this location, OMI inferred concentrations were

**Table 3.** Mean surface-to-column ratio ( $\pm 95\%$  confidence interval) and characteristic height, by season.

Season	Mean surface-to-column ratio ( $\pm 95\%$ CI) (ppb/ $1 \times 10^{15}$ molec cm <sup>-2</sup> )	Mean characteristic height (m)
Winter	2.0 ( $\pm 0.41$ )	210
Spring	1.7 ( $\pm 0.13$ )	245
Summer	0.94 ( $\pm 0.07$ )	450
Autumn	0.81 ( $\pm 0.07$ )	525

5.4 ppb higher, on average, than the concentrations measured by this passive monitor.

These two extreme situations highlight some of the limitations of this approach. Using a CTM to provide a better estimate of the free-tropospheric column and applying Eq. (4) of Lamsal et al. (2008) could potentially lead to improvements in the surface NO<sub>2</sub> estimates, especially in rural areas. Another possible approach would be to empirically determine a spatially varying surface-to-column ratio, by fitting a polynomial surface to interpolate the measured point values. However, for this approach to work, a higher density in situ monitoring network would be required to capture the variability and to account for the uncertainty in each individual surface-to-column measurement. The simplest step towards improving the inference of ground-based NO<sub>2</sub> from OMI data would be to increase the proportion of NO<sub>2</sub> monitoring locations at rural sites.

### 3.3.2 Temporal patterns

Temporal patterns in the OMI data and inferred ground-based concentrations were explored to illustrate the application of this methodology. The patterns examined included the variation in inferred concentrations across the region over four years, and the seasonality in the surface-to-column ratio. Over a span of 4 yr, using only the 5 permanent MoE monitoring stations, the seasonal average surface-to-column ratio was found to vary from a minimum of 0.81 ppb/ $1 \times 10^{15}$  molec cm<sup>-2</sup> ( $H = 525$  m) in the autumn and a maximum of 2.0 ppb/ $1 \times 10^{15}$  molec cm<sup>-2</sup> ( $H = 210$  m) in the winter (Table 3). No significant relationship with characteristic height was found for any meteorological variable. However, Lake Erie's water temperature normally follows a very similar seasonal trend, with winter and spring (December through May) having lower lake temperatures than summer and autumn (June through November) (NOAA, 2010). Therefore, it appears that higher lake temperatures in the summer and autumn may be driving the vertical mixing of NO<sub>2</sub> in the region, as seen in the seasonal pattern in characteristic height.

In order to verify the validity of the surface NO<sub>2</sub> procedure developed from the BAQS-Met period for use over longer time spans, we calculated two week average OMI-derived

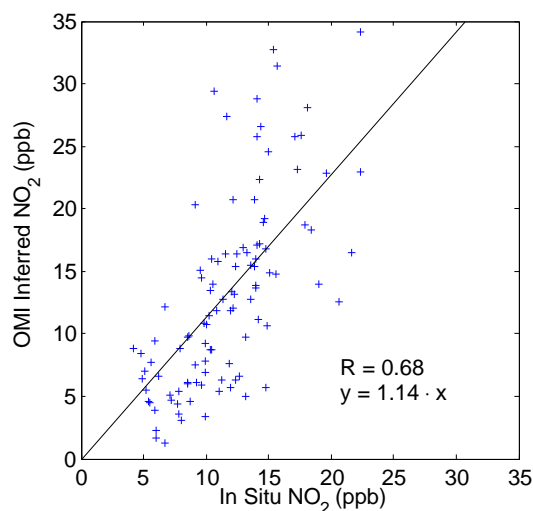


**Fig. 10.** Two-week average OMI inferred surface NO<sub>2</sub> vs. in situ CL NO<sub>2</sub> measurements for 2005–2009. Improvement in correlation ( $R = 0.61$  for DOMINO columns vs. in situ) was mainly due to a few periods in winter months, which showed greater agreement after the inference method was applied.

surface-level NO<sub>2</sub> concentrations using only 4 of the 5 available permanent MoE monitoring sites, retaining the last site for evaluation. For this purpose, two week averages were calculated for both in situ CL measured NO<sub>2</sub> concentration at the hold-back site and OMI-inferred NO<sub>2</sub> concentration for the nearest 0.1° grid cell. This procedure was done for every 2-week period from January 2005 to December 2009, randomly changing which site was held back each time. Surface inferred OMI concentrations showed a stronger correlation ( $R = 0.68$ , Fig. 10) with in-situ CL-measured 2-week averages than OMI column values ( $R = 0.61$ ). This provides confidence that the inference method is applicable to other periods (i.e., not just the summer 2007 BAQS-met campaign period), continuing to add skill to the estimates of surface NO<sub>2</sub>. This improvement (i.e. increase in correlation) is largely due to a few specific periods which appear to benefit the most from the inference method. These periods all occurred between the months of November and March, and were observed across all 5 yr. These months tend to have more pixels excluded due to clouds and snow. Column averages calculated from fewer overpasses would suffer more from day-to-day variations in the surface-to-column ratio, whereas our method removes this influence from each overpass. Furthermore, OMI NO<sub>2</sub> retrievals are expected to be biased over snow (O'Byrne et al., 2010); our approach empirically corrects for that bias.

As an illustrative example, Fig. 11 provides regional snapshots of OMI-inferred surface NO<sub>2</sub> concentrations for 4 yr. From 2006 to 2009, OMI-inferred NO<sub>2</sub> in the region displayed a slow decline in and around the industrial areas on both sides of the border overall, with a sudden drop in the

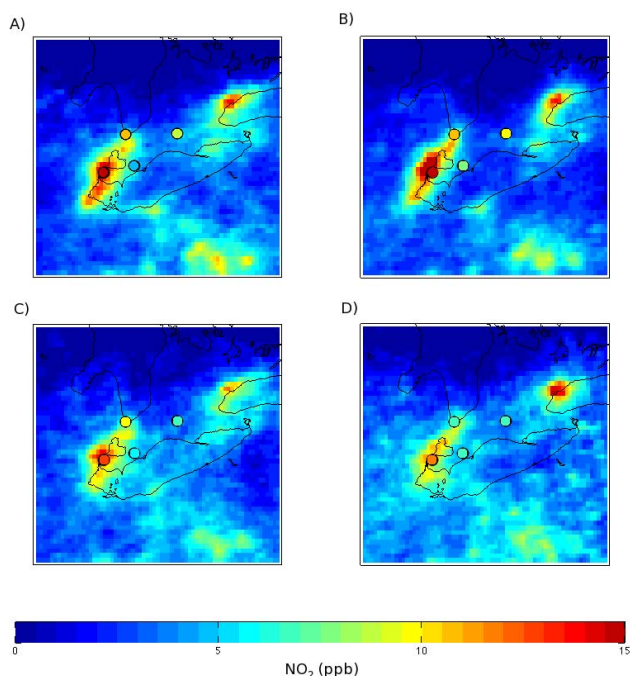


**Fig. 11.** OMI inferred NO<sub>2</sub> concentrations for summers of (A) 2006, (B) 2007, (C) 2008 and (D) 2009. Colour circles represent average in situ measurements over the same time periods, on the same colour scale as the maps.

summer of 2009. This decrease in regional NO<sub>2</sub> concentrations may have coincided with a drop in manufacturing in the area during the economic slowdown after the fall of 2008. Concentrations over the West end of Lake Erie remained fairly stable in comparison with concentrations onshore nearby, indicating that meteorologically driven dispersion of NO<sub>2</sub> remained constant over 3 of the 4 yr in question.

### 3.3.3 Spatial patterns

Figure 12 shows average OMI inferred surface NO<sub>2</sub> concentrations for the entire 2007 year separated by wind direction. It is important to acknowledge the implicit assumption that exclusion of some days due to clouds does not introduce any bias in the maps. The long term comparison using the leave-one-out approach indicates that this is true, in general. It is possible, however, that, when separating overpasses by wind direction, we are exposing systematic errors which are masked by combining all overpasses. That is, if cloudy days from the southeast direction are cleaner than clear days and if cloudy days from the southwest direction are more polluted than clear days, by combining the days from both of these directions the errors cancel each other out. Also, it should be pointed out that the same single surface-to-column ratio calculated for the BAQS-met study area was applied across the entire range of the maps. The error introduced by this assumption may grow as the distance from the original points

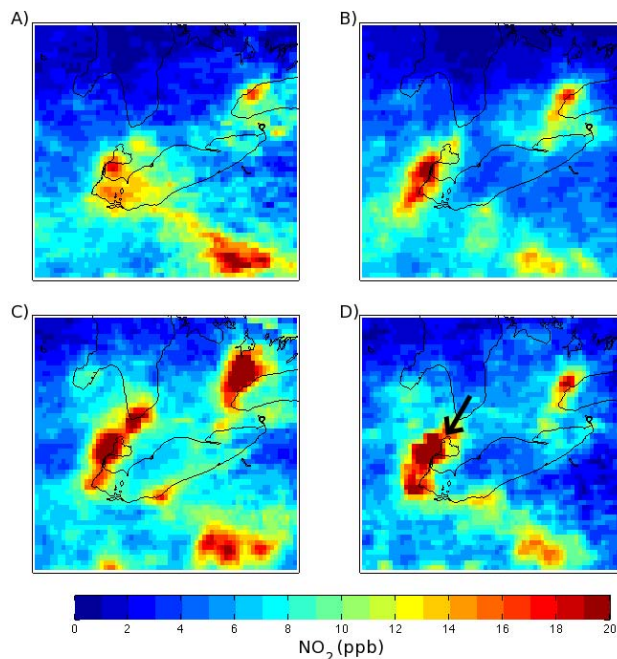


**Fig. 12.** OMI inferred NO<sub>2</sub> concentrations for 2007 grouped by surface wind direction as measured at Windsor. (A) represents only OMI measurements taken when wind was blowing from the NW direction. (B, C and D) Same as (A) but NE, SW and SE directions, respectively. NW coast of Lake St. Clair indicated by black arrow in (D); inferred concentrations over the lake are approximately half those onshore when the lake is upwind of the onshore emissions sources (i.e. when the wind blows from the SE). Number of overpasses used to generate each average was 21 (21 % of available overpasses) for (A), 70 for (B), 98 for (C) and 48 for (D). The total number of overpasses used is less than the total number of days in the year because of rejection of overpasses for which > 2 surface stations were occluded by clouds.

of calculation grows and therefore what appear to be large differences between wind directions around the Toronto area (Northeast corner of the maps) could in fact be errors introduced by this assumption.

Figure 12d includes OMI measurements when the wind was blowing from due East to due South directions. This quadrant was particularly important to the study of the region because it illustrated the impact of easterly airflows nearly perpendicularly across the Canada-US border at Windsor-Detroit, thus highlighting any NO<sub>x</sub> emissions sources on the Canadian side. The sharpness of the boundary can be observed on the NW shore of Lake St Clair (marked by a black arrow in Fig. 12d): over the lake the column measures approximately half those immediately adjacent the lake on the NW shore.

In order to more clearly see the effects of wind direction on surface level NO<sub>2</sub> concentrations, Fig. 13 shows the difference between the average concentration grouped by wind direction and the annual average concentration (all

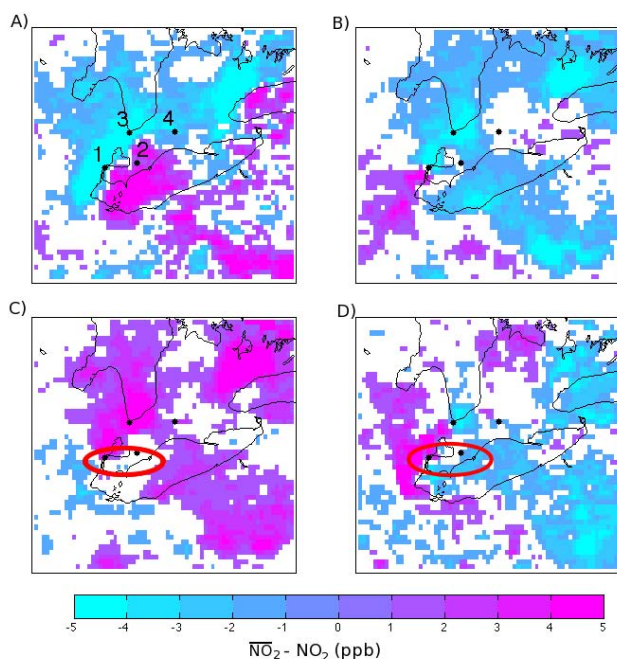


**Fig. 13.** Difference between OMI inferred NO<sub>2</sub> grouped by wind direction and annual average OMI inferred NO<sub>2</sub>. Purple (positive), indicates higher than average NO<sub>2</sub> concentrations when the wind blows from that direction while blue indicates lower than average concentrations. Uncoloured regions are less than 1 ppb difference. Labeled points in (A) represent surface monitoring stations (1: WW and WD; 2: CH; 3: SA; 4: LO) (A) represents only OMI measurements taken when wind was blowing from the NW direction. (B, C and D) Same as (A) but NE, SW and SE directions, respectively. See text for in-depth description regarding marked areas in (C) and (D).

wind directions). Overall, NO<sub>2</sub> concentrations were higher when the wind blew from the SE and SW. Looking at the campaign area, the area between Lake Erie and Lake St. Clair (circled in red in Fig. 13c, d), a different pattern emerges: the area remains relatively unaffected by wind direction except for markedly elevated NO<sub>2</sub> concentrations across the entire region, as well as the west end of Lake Erie, when the wind blows from the NW. Good agreement between the satellite-derived, wind-direction-dependent concentrations and in-situ, wind-direction-dependent concentrations was also found.

It should also be possible to discern areas of intense emissions from the difference maps. Indeed, the core of Detroit/Windsor, near the Ambassador Bridge over the Detroit River, is consistently found to be a boundary between below average and above average concentrations, for all wind directions (Fig. 13). Another area of interest is the area to the north of Lake St. Clair, just south of Sarnia where a large power generation station is situated in Ontario, as well as several emissions sources on the US side. Outflow can be seen from Cleveland, on the south side of Lake Erie, especially over the lake when wind flows from the SW.

## 4 Conclusions

We have shown that utilization of empirically calculated surface-to-column ratios in conjunction with OMI satellite NO<sub>2</sub> column measurements can provide reasonable long-term surface concentrations at a regional-to-local scale (~11 km resolution). The approach leads to useful information on spatial and temporal variations in surface NO<sub>2</sub>, if sufficient in situ measurements (average monitor spacing <100 km) are available for the region. This approach has the advantage of providing an empirical correction for the bias in OMI NO<sub>2</sub> retrievals.

We showed that this method can be exploited to examine the extent of outflow of urban air pollution at a regional scale. Significant contributions to rural NO<sub>2</sub> pollution in Southwestern Ontario were displayed when wind flowed from the NW direction, due to outflow from the Windsor-Detroit area. These examples have shown how future work using these types of maps in qualitative and quantitative analyses such as population exposure assessment and model evaluation, could be conducted.

NO<sub>z</sub> interference was quantified using collocated monitors and it was shown that intake line adsorption and desorption contribute to both the magnitude of this interference and its temporal smoothing. Because of this smoothing, the effects of high midday ratios of (NO<sub>2</sub>)<sub>m</sub>/NO<sub>2</sub>, driven largely by low midday NO<sub>2</sub> values, can be mitigated by using whole-day averages.

It should be noted that, although the long term results were calculated using only the urban monitoring stations permanently maintained by the Ontario Ministry of the Environment, comparison of OMI inferred NO<sub>2</sub> concentrations to campaign passive monitoring data showed a slope much closer to one when rural monitoring locations were also included. This was attributed mainly to the situation of permanent monitoring stations near sources, making these point sources less representative of the entire spatial footprint represented by a single OMI pixel measurement of the same location. It may be sensible, therefore, in future to allocate more monitoring resources to rural areas, where spatial distribution of NO<sub>2</sub> is less heterogeneous, to aid in interpretation of satellite results, which can yield significant insights into regional scale air quality.

*Acknowledgements.* We would like to thank the Canadian Foundation for Climate and Atmospheric Sciences for funding for this study and the Ontario Ministry of the Environment for providing NO<sub>2</sub> data and support for the BAQS-met campaign, and Sandy Benetti for conducting the passive sampling field work and IC analysis.

Edited by: R. McLaren

## References

- Arain, M. A., Blair, R., Finkelstein, N., Brook, J., and Jerrett, B.: Meteorological influences on the spatial and temporal variability of NO<sub>2</sub> in Toronto and Hamilton, *Can. Geogr.-Geogr. Can.*, 53, 165–190, 2009.
- Boersma, K., Eskes, H., and Brinksma, E.: Error analysis for tropospheric NO<sub>2</sub> retrieval from space, *J. Geophys. Res.-Atmos.*, 109, D04311, doi:10.1029/2003JD003962, 2004.
- Boersma, K. F., Eskes, H. J., Veefkind, J. P., Brinksma, E. J., van der A, R. J., Sneep, M., van den Oord, G. H. J., Levelt, P. F., Stammes, P., Gleason, J. F., and Bucsela, E. J.: Near-real time retrieval of tropospheric NO<sub>2</sub> from OMI, *Atmos. Chem. Phys.*, 7, 2103–2118, doi:10.5194/acp-7-2103-2007, 2007.
- Boersma, K. F., Jacob, D. J., Bucsela, E. J., Perring, A. E., Dirksen, R., van der A, R. J., Yantosca, R. M., Park, R. J., Wenig, M. O., Bertram, T. H., and Cohen, R. C.: Validation of OMI tropospheric NO<sub>2</sub> observations during INTEX-B and application to constrain NO<sub>x</sub> emissions over the Eastern United States and Mexico, *Atmos. Environ.*, 42, 4480–4497, doi:10.1016/j.atmosenv.2008.02.004, 2008.
- Boersma, K. F., Jacob, D. J., Trainic, M., Rudich, Y., DeSmedt, I., Dirksen, R., and Eskes, H. J.: Validation of urban NO<sub>2</sub> concentrations and their diurnal and seasonal variations observed from the SCIAMACHY and OMI sensors using in situ surface measurements in Israeli cities, *Atmos. Chem. Phys.*, 9, 3867–3879, doi:10.5194/acp-9-3867-2009, 2009.
- Bovensmann, H., Burrows, J. P., Buchwitz, M., Frerick, J., Noel, S., Rozanov, V. V., Chance, K., and Goede, A. P. H.: SCIAMACHY: mission objectives and measurement modes, *J. Atmos. Sci.*, 56, 127–150, 1999.
- Brook, J. R., Burnett, R. T., Dann, T. F., Cakmak, S., Goldberg, M. S., Fan, X., and Wheeler, A. J.: Further interpretation of the acute effect of nitrogen dioxide observed in Canadian time-series studies, *J. Expo. Sci. Env. Epid.*, 17, S36–S44, doi:10.1038/sj.jes.7500626, 2007.
- Bucsela, E., Celarier, E., Wenig, M., Gleason, J., Veefkind, J., Boersma, K., and Brinksma, E.: Algorithm for NO<sub>2</sub> vertical column retrieval from the Ozone Monitoring Instrument, *IEEE T. Geosci. Remote*, 44, 1245–1258, doi:10.1109/TGRS.2005.863715, 2006.
- Bucsela, E. J., Perring, A. E., Cohen, R. C., Boersma, K. F., Celarier, E. A., Gleason, J. F., Wenig, M. O., Bertram, T. H., Wooldridge, P. J., Dirksen, R., and Veefkind, J. P.: Comparison of tropospheric NO<sub>2</sub> from in situ aircraft measurements with near-real-time and standard product data from OMI, *J. Geophys. Res.-Atmos.*, 113, D16S31, doi:10.1029/2007JD008838, 2008.
- Burrows, J., Weber, M., Buchwitz, M., Rozanov, V., Ladstätter-Weissenmayer, A., Richter, A., DeBeek, R., Hoogen, R., Bramsteadt, K., Eichmann, K., Eisinger, M., and Perner, D.: The Global Ozone Monitoring Experiment (GOME): mission concept and first scientific results, *J. Atmos. Sci.*, 56, 151–175, 1999.
- Celarier, E. A., Brinksma, E. J., Gleason, J. F., Veefkind, J. P., Cede, A., Herman, J. R., Ionov, D., Goutail, F., Pommereau, J. P., Lambert, J. C., van Roozendaal, M., Pinardi, G., Wittrock, F., Schönhardt, A., Richter, A., Ibrahim, O. W., Wagner, T., Borkov, B., Mount, G., Spinei, E., Chen, C. M., Pongetti, T. J., Sander, S. P., Bucsela, E. J., Wenig, M. O., Swart, D. P. J., Volten, H., Kroon, M., and Levelt, P. F.: Validation of Ozone Monitoring Instrument nitrogen dioxide columns, *J. Geophys. Res.*, 113, D15S15, doi:10.1029/2007JD008908, 2008.
- Clark, N. A., Demers, P. A., Karr, C. J., Koehoorn, M., Lencar, C., Tamburic, L., and Brauer, M.: Effect of early life exposure to air pollution on development of childhood asthma, *Environ. Health Persp.*, 118, 284–290, doi:10.1289/ehp.0900916, 2010.
- Hains, J. C., Boersma, K. F., Kroon, M., Dirksen, R. J., Cohen, R. C., Perring, A. E., Bucsela, E., Volten, H., Swart, D. P. J., Richter, A., Wittrock, F., Schönhardt, A., Wagner, T., Ibrahim, O. W., van Roozendaal, M., Pinardi, G., Gleason, J. F., Veefkind, J. P., and Levelt, P.: Testing and improving OMI DOMINO tropospheric NO<sub>2</sub> using observations from the DANDELIONS and INTEX-B validation campaigns, *J. Geophys. Res.-Atmos.*, 115, D05301, doi:10.1029/2009JD012399, 2010.
- Halla, J. D., Wagner, T., Beirle, S., Brook, J. R., Hayden, K. L., O'Brien, J. M., Ng, A., Majonis, D., Wenig, M. O., and McLaren, R.: Determination of tropospheric vertical columns of NO<sub>2</sub> and aerosol optical properties in a rural setting using MAX-DOAS, *Atmos. Chem. Phys. Discuss.*, 11, 13035–13097, doi:10.5194/acpd-11-13035-2011, 2011.
- Herron-Thorpe, F. L., Lamb, B. K., Mount, G. H., and Vaughan, J. K.: Evaluation of a regional air quality forecast model for tropospheric NO<sub>2</sub> columns using the OMI/Aura satellite tropospheric NO<sub>2</sub> product, *Atmos. Chem. Phys.*, 10, 8839–8854, doi:10.5194/acp-10-8839-2010, 2010.
- Jerrett, M., Finkelstein, M. M., Brook, J. R., Arain, M. A., Kanaroglou, P., Stieb, D. M., Gilbert, N. L., Verma, D., Finkelstein, N., Chapman, K. R., and Sears, M. R.: A cohort study of traffic-related air pollution and mortality in Toronto, Ontario, Canada, *Environ. Health Persp.*, 117, 772–777, doi:10.1289/ehp.11533, 2009.
- Kim, S. W., Heckel, A., Frost, G. J., Richter, A., Gleason, J., Burrows, J. P., McKeen, S., Hsie, E. Y., Granier, C., and Trainer, M.: NO<sub>2</sub> columns in the Western United States observed from space and simulated by a regional chemistry model and their implications for NO<sub>x</sub> emissions, *J. Geophys. Res.*, 114, D11301, doi:10.1029/2008JD011343, 2009.
- Kramer, L. J., Leigh, R. J., Remedios, J. J., and Monks, P. S.: Comparison of OMI and ground-based in situ and MAX-DOAS measurements of tropospheric nitrogen dioxide in an urban area, *J. Geophys. Res.-Atmos.*, 113, D16S39, doi:10.1029/2007JD009168, 2008.
- Lamsal, L. N., Martin, R. V., van Donkelaar, A., Steinbacher, M., Celarier, E. A., Bucsela, E., Dunlea, E. J., and Pinto, J. P.: Ground-level nitrogen dioxide concentrations inferred from the satellite-borne Ozone Monitoring Instrument, *J. Geophys. Res.-Atmos.*, 113, D16308, doi:10.1029/2007JD009235, 2008.
- Lamsal, L. N., Martin, R. V., van Donkelaar, A., Celarier, E. A., Bucsela, E. J., Boersma, K. F., Dirksen, R., Luo, C., and Wang, Y.: Indirect validation of tropospheric nitrogen dioxide retrieved from the OMI satellite instrument: insight into the seasonal variation of nitrogen oxides at northern midlatitudes, *J. Geophys. Res.-Atmos.*, 115, D05302, doi:10.1029/2009JD013351, 2010.
- Lenters, V., Uiterwaal, C. S., Beelen, R., Bots, M. L., Fischer, P., Brunekreef, B., and Hoek, G.: Long-term exposure to air pollution and vascular damage in young adults, *Epidemiology*, 21, 512–520, doi:10.1097/EDE.0b013e3181dec3a7, 2010.
- Levelt, P., van den Oord, G., Dobber, M., Malkki, A., Visser, H.,

- de Vries, J., Stammes, P., Lundell, J., and Saari, H.: The Ozone Monitoring Instrument, *IEEE T. Geosci. Remote*, 44, 1093–1101, doi:10.1109/TGRS.2006.872333, 2006.
- Levy, I., Makar, P. A., Sills, D., Zhang, J., Hayden, K. L., Michele, C., Narayan, J., Moran, M. D., Sjostedt, S., and Brook, J.: Unraveling the complex local-scale flows influencing ozone patterns in the southern Great Lakes of North America, *Atmos. Chem. Phys.*, 10, 10895–10915, doi:10.5194/acp-10-10895-2010, 2010.
- Makar, P. A., Gong, W., Mooney, C., Zhang, J., Davignon, D., Samaali, M., Moran, M. D., He, H., Tarasick, D. W., Sills, D., and Chen, J.: Dynamic adjustment of climatological ozone boundary conditions for air-quality forecasts, *Atmos. Chem. Phys.*, 10, 8997–9015, doi:10.5194/acp-10-8997-2010, 2010.
- Martin, R. V., Chance, K., Jacob, D. J., Kurosu, T. P., Spurr, R. J. D., Bucsel, E., Gleason, J. F., Palmer, P. I., Bey, I., Fiore, A. M., Li, Q., Yantosca, R. M., and Koelemeijer, R. B. A.: An improved retrieval of tropospheric nitrogen dioxide from GOME, *J. Geophys. Res.*, 107, 4437, doi:10.1029/2001JD001027, 2002.
- MoE: Air Quality in Ontario 2008 Report, available at: <http://www.ene.gov.on.ca/publications/7356e.pdf> (last access: August 2010), 2008.
- NOAA: Lake Erie Temperature Normals, available at: <http://www.erh.noaa.gov/buf/laketemps/lktemp.html> (last access: December 2010), 2010.
- O’Byrne, G., Martin, R. V., van Donkelaar, A., Joiner, J., and Celarier, E. A.: Surface reflectivity from the Ozone Monitoring Instrument using the Moderate Resolution Imaging Spectroradiometer to eliminate clouds: effects of snow on ultraviolet and visible trace gas retrievals, *J. Geophys. Res.*, 115, D17305, doi:10.1029/2009JD013079, 2010.
- Ordóñez, C., Richter, A., Steinbacher, M., Zellweger, C., Nuss, H., Burrows, J., and Prevot, A.: Comparison of 7 years of satellite-borne and ground-based tropospheric NO<sub>2</sub> measurements around Milan, Italy, *J. Geophys. Res.-Atmos.*, 111, D05310, doi:10.1029/2005JD006305, 2006.
- Russell, A. R., Valin, L. C., Bucsel, E. J., Wenig, M. O., and Cohen, R. C.: Space-based constraints on spatial and temporal patterns of NO<sub>x</sub> emissions in California, 2005–2008, *Environ. Sci. Technol.*, 44, 3608–3615, doi:10.1021/es903451j, 2010.
- Ryerson, T., Williams, E., and Fehsenfeld, F.: An efficient photolysis system for fast-response NO<sub>2</sub> measurements, *J. Geophys. Res.-Atmos.*, 105, 26447–26461, 2000.
- Statistics Canada: 2006 Census of Canada Census Profiles Marital status, common-law status, families, dwellings, and households Tables: Profile of Marital Status, Common-law Status, Families, Dwellings and Households, for Census Metropolitan Areas and Census Agglomerations, 2006 Census., Tech. rep., Statistics Canada, 2006.
- Steinbacher, M., Zellweger, C., Schwarzenbach, B., Bugmann, S., Buchmann, B., Ordóñez, C., Prevot, A. S. H., and Hueglin, C.: Nitrogen oxide measurements at rural sites in Switzerland: Bias of conventional measurement techniques, *J. Geophys. Res.-Atmos.*, 112, D11307, doi:10.1029/2006JD007971, 2007.
- US Census Bureau: Table 1. Annual Estimates of the Population of Metropolitan and Micropolitan Statistical Areas: 1 April 2000 to 1 July 2009 (CBSA-EST2009-01), available at: <http://www.census.gov/popest/metro/CBSA-est2009-annual.html> (last access: October 2010), 2010.
- Wenig, M., Cede, A., Bucsel, E., Celarier, E., Boersma, K., Veeffkind, J., Brinkma, E., Gleason, J., and Herman, J.: Validation of OMI tropospheric NO<sub>2</sub> column densities using direct-Sun mode Brewer measurements at NASA Goddard Space Flight Center, *J. Geophys. Res.-Atmos.*, 113, D16S45, doi:10.1029/2007JD008988, 2008.
- Winer, A., Peters, J., Smith, J., and Pitts, J.: Response Of Commercial Chemiluminescent NO-NO<sub>2</sub> Analyzers To Other Nitrogen-Containing Compounds, *Environ. Sci. Technol.*, 8, 1118–1121, doi:10.1021/es60098a004, 1974.